Traffic & Transportation

A Reliability-Based Network Equilibrium Model with Electric Vehicles and Gasoline Vehicles

Qiang TU[1], Manman LI[2], Yongjun WU[3]

Original Scientific Paper
Submitted: 16 Feb. 2023
Accepted: 27 Oct. 2023

[1] Corresponding author, dqtu_1991@163.com, School of Traffic and Transportation, Chongqing Jiaotong University; Engineering Research Center for Waste Oil Recovery Technology and Equipment, Ministry of Education, Chongqing Technology and Business University; Chongqing Urban Investment Gold Card Information Industry (Group) Co. Ltd.

[2] limanman@chd.edu.cn, School of Automobile, Chang 'an University

[3] yongjunwu@cqjtu.edu.cn, School of Traffic and Transportation, Chongqing Jiaotong University

Publisher:
Faculty of Transport and Traffic Sciences, University of Zagreb

ABSTRACT

With the popularity of electric vehicles, they have become an indispensable part of traffic flow on the road network. This paper presents a reliability-based network equilibrium model to realise the traffic flow pattern prediction on the road network with electric vehicles and gasoline vehicles, which incorporates travel time reliability, electric vehicles' driving range and recharge requirement. The mathematical expression of reliable path travel time is derived, and the reliability-based network equilibrium model is formulated as a variational inequality problem. Then a multi-criterion labelling algorithm is proposed to solve the reliable shortest path problem, and a column-generation-based method of the successive average algorithm is proposed to solve the reliability-based network equilibrium model. The applicability and efficiency of the proposed model and algorithm are verified on the Nguyen-Dupuis network and the real road network of Sioux Falls City. The proposed model and algorithm can be extended to other road networks and help traffic managers analyse traffic conditions and make sustainable traffic policies.

KEYWORDS

transportation engineering; reliability-based network equilibrium; electric vehicle; driving range; recharge requirement.

1. INTRODUCTION

With the increased attention to traffic consumption and carbon emissions, electric vehicles (EVs) with low energy consumption and low emissions have been actively promoted worldwide [1]. According to the latest Global Electric Vehicle Outlook (2022) released by the International Energy Agency (IEA), the global sales of EVs doubled in 2021 compared to the previous year to a new record of 6.6 million, and the total number of EVs on the world's roads up to about 16.5 million [2]. More than 30 countries, states and cities have announced their timetables of future gasoline/diesel vehicle bans [3]. In addition, at least 6 major automakers have pledged to work toward phasing out sales of new gasoline/diesel vehicles by 2040 worldwide. For example, Hainan province in China plans to ban the sale of gasoline vehicles (GVs) by 2030 [4], and BYD was the first automaker in the world to officially announce the cessation of GV production on 5 April 2022. The electrification of urban transportation will have a lasting impact on the transportation system, and the traffic flow on the road network will be a mixed flow of conventional GVs and EVs for a long term [5].

Predicting traffic flow patterns on the road network remains a hot subject in the field of sustainable transportation, which can help traffic managers and planners analyse traffic conditions and make sustainable traffic policies [6, 7]. The traffic assignment problem (TAP) based on the network equilibrium model has been the predominant method to predict traffic flow patterns on the road network since the Wardrop principle was proposed [8]. The famous Wardrop's first principle known as "user equilibrium" (UE) describes such a traffic equilibrium condition that the travel time of all used paths for each origin-destination (O-D) pair is shorter than or equal to that of unused paths, and no traveller can improve their travel time by unilaterally changing paths in this state [9]. Building upon the basic UE principle, numerous extensions and variations have been developed to address specific complexities and nuances in network equilibrium modelling, including stochastic user

equilibrium [10, 11], dynamic user equilibrium [12], reliability-based network equilibrium [13, 14], multiclass network equilibrium [15], multimodal network equilibrium [16] etc.

In the UE and other extended network equilibrium models, traffic demand is assigned to the transportation network based on travellers' path choice behaviour. Therefore, travellers' path choice behaviour is the critical and fundamental process in building a network equilibrium model. To predict the traffic flow pattern of the transportation network with EVs, it is important to understand their path choice behaviour. EV travellers' path choice behaviour is often considered different from that of GV travellers due to range anxiety, en-route recharge requirements and insufficient charging infrastructure [17, 18]. For example, EVs may opt for detours to pass by charging stations in order to avoid running out of charge. In other words, the path chosen by EV travellers may include detours and recharging actions with the consideration of driving range limits and recharge requirements. Due to the different path choice behaviour, the conventional network equilibrium model needs to be rebuilt to apply to the transportation network with both EVs and GVs. Recent network equilibrium models involving EVs can be divided into three categories according to EV travel characteristics.

The first category incorporates EVs' environmental cost or operation cost into the network equilibrium models. Researchers believe that EV and GV travellers are different in terms of environmental awareness, and their travel costs are different in energy consumption and pollution emissions even when travelling the same path. Ma et al. incorporated the environmental cost into the travel cost function and built a stochastic user equilibrium model to analyse how the environmental cost affects the network utilities. They also extended it to the condition with elastic demand [19, 20]. Ahn et al. developed and investigated the impact of a multi-objective user equilibrium on a large-scale city network considering the difference in energy consumption of EVs and GVs [21]. Ma et al. proposed a stochastic user equilibrium model considering the different operation costs of EVs and GVs to analyse the adoption of EVs in an urban transportation network [22]. These studies have been conducted on urban transportation networks for EVs' intra-city travel, and EVs' driving range limits and recharging requirements are not considered.

The second category takes into account EVs' distance limit or range anxiety due to limited driving range. Jiang et al. built a path-constrained network equilibrium model, in which the distance-limited constraint of EVs was introduced into the UE model [23, 24]. Jing et al. proposed a stochastic user equilibrium model with a distance limit considering the perceived error of travellers and applied it to optimise the charging station location [25, 26]. Yan and Guo proposed a multiclass cumulative prospect theory-based stochastic user equilibrium model with path constraints in a degradable transportation network to handle jointly the range anxiety issue and the perfectly rational issue [15]. Li et al. built a day-to-day traffic assignment model to investigate the effect of the use of battery electric vehicles on traffic dynamics [5]. The limitation of these studies is that they do not take into account the recharging requirement of EVs.

The third category incorporates both limited driving range and recharge requirement into network equilibrium models. Xie et al. built the network equilibrium considering both factors of driving range limits and recharge requirements. Their results showed that both factors have a great influence on the traffic flow pattern on the road network [27]. He et al. assumed EV drivers select paths to minimise their driving times while ensuring not running out of charge and formulated three mathematical models to describe the network equilibrium of EVs, in which the recharging time and flow-dependent energy were considered [28]. Xu et al. developed a nonlinear minimisation model for mixed battery electric and gasoline vehicles in a transportation network with battery swapping stations by incorporating flow-dependent dwell time and effects of road grade on electricity consumption rate [29]. Zhang developed a novel convex programming formulation for a mixed-vehicular traffic assignment accounting for en-route multi-modal recharge, and EVs' path choices were represented as a resource-constrained shortest path subproblem with recharge time [30].

The studies above mainly focus on the effect of EVs' travel characteristics on path choice. However, the effect of travel time variation caused by unpredictable perturbations in the transportation network on path choice is significant and cannot be overlooked. Travel time reliability is a key indicator to reflect the travel time variation in the context of an uncertain transportation network, which is defined as the probability that travellers can reach destinations within a certain travel time [31, 32]. Facing the uncertainty of travel time, travellers focus not only on expected travel time but also travel time reliability when making path choices [33]. Some research found that the value of reliability is close to or even higher than the value of travel time, and travel time reliability needs to be incorporated into the cost function of path choice models [34]. For EV travellers,

path travel time uncertainty comes from both travel time uncertainty on roads and dwell time uncertainty at charging infrastructure caused by uncertain traffic flow and charging flow. Therefore, EV travellers may care more about travel time reliability than GV travellers. Recent researchers have paid attention to the effect of travel time reliability on the path choice of EV travellers, which is called the reliable shortest path problem for EVs. Tu et al. studied the constrained reliable shortest path problem for EVs in an urban transportation network [35]. Ruß et al. further studied the constrained reliable shortest path problem on stochastic time-dependent networks [36]. Shen et al. reformulated such a problem as a bi-objective model in which one objective is reliable travel time and the other is the energy consumption of EVs [37]. However, the reliable shortest path problem for EVs with driving range limits and recharge requirements remains a challenge, and few studies have focused on the corresponding network equilibrium problems.

Considering travel time reliability, EVs' driving range and recharge requirements, this paper aims to propose a reliability-based network equilibrium model to predict the traffic flow pattern on the road network with EVs and GVs. In this model, reliable travel time is adopted to treat travel time and travel time reliability, which is derived as expected travel time plus a safety margin, and the safety margin is calculated according to travel time distribution and confidence level. Integrating travel time reliability into the network equilibrium model with EVs and GVs fills the research gaps, and our main contributions are summarised as follows:

1) We derived the reliable path travel time with the consideration of uncertain traffic demand as the source and formulated the reliability-based network equilibrium model with EVs and GVs as a variational inequality problem.
2) We proposed a multi-criterion labelling algorithm to solve the reliable shortest path problem and incorporated the method of a successive average (MSA) algorithm into a column generation framework to solve the reliability-based network equilibrium model.
3) We tested the proposed model and algorithm on the Nguyen-Dupuis network and Sioux Falls network. Results comparison and a sensitivity analysis were carried out to illustrate the essential ideas of the proposed model. Due to the Sioux Falls network being a real city network, the applicability of the proposed algorithm was also verified.

The remainder of the paper is organised as follows. Section 2 formulates the reliability-based network equilibrium model. Section 3 introduces the solution procedure to solve the formulated model. Section 4 provides two numerical examples to illustrate the proposed model and algorithm. Section 5 concludes the study and suggests future research directions.

2. MODEL FORMULATION

Similar to previous studies, the uncertainty of travel time is assumed to mainly come from the stochastic traffic demand in this paper [13, 38, 39]. Some basic assumptions should be listed before modelling:

1) The traffic demand of the origin-destination (O-D) pair (i.e. O-D traffic demand) follows the lognormal distribution, and the variance-to-mean ratio is denoted as ρ^w for O-D pair w;
2) The path flows follow the same probability distribution as the corresponding O-D traffic demand and have the same variance-to-mean ratio;
3) The path flows are mutually independent;
4) The link travel time and dwell time at charging infrastructure are mutually independent.

These four assumptions are necessary to derive the flow distribution and reliable path travel time in the following sections 2.1.1 and 2.1.4. Similar assumptions can be also found in the literature related to the reliability-based network equilibrium models [13, 38–40].

It is noted that there are mainly 3 types of charging infrastructure, namely the AC charging pile, charging station and battery swapping station (BSS) [41]. For long-distance travel, the dwell time of en-route recharge is an important part of path travel time. The dwell time consists of waiting time and service time at charging infrastructure. The waiting time is affected by queue length and service time, and service time mainly depends on the type of charging facility for a certain recharge amount. Up to now, the service time at BSSs is considered to be the shortest, and it can achieve energy refuelling in a short time parallel to GVs [42]. In the future, with the development of fast charging technology, the fast-charging station is likely to provide a similar fast service experience to that of the BSS. Based on these reasons, the BSS is chosen as the charging infrastructure to build our model.

2.1 Derivation of reliable path travel time

In the network equilibrium model, the path travel time is the determining factor affecting travellers' path choice. Taking the stochastic traffic demand as the source, the mathematical expression of a reliable path travel time needs to be derived. According to the transfer process of variables, the derivation process of a reliable path travel time can be summarised as the following *Figure 1*.

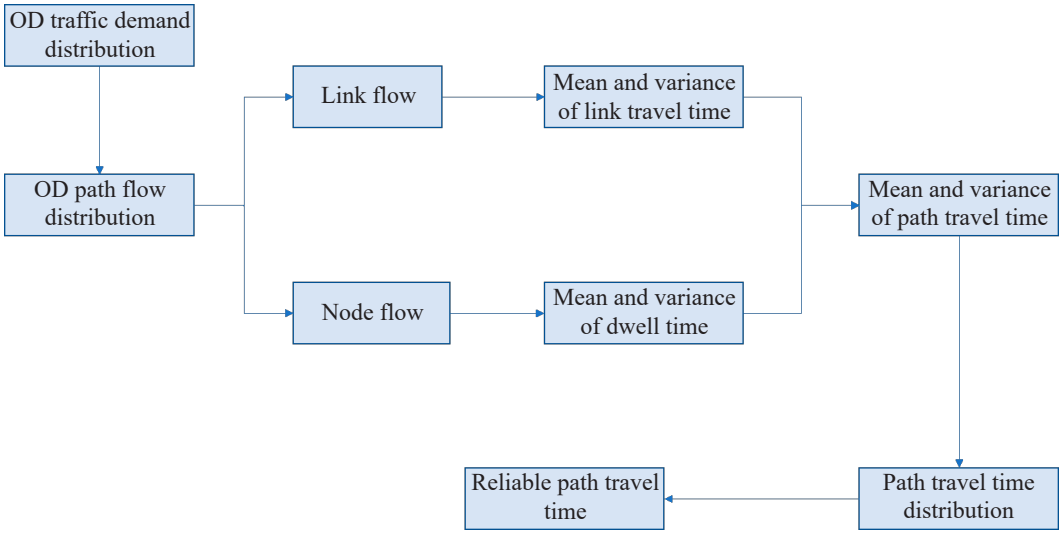

Figure 1 – The derivation process of reliable path travel time

Let Q^w be the traffic demand between O-D pair w, F_k^w be the traffic flow on path k between O–D pair w, X_a be the traffic flow on link a, and X_i be the traffic flow at BSS node i. It is worth noting that Q^w, F_k^w, X_a and X_i are all stochastic variables. Based on the assumptions 1–3, the O–D traffic demands follow the lognormal distribution, and the distribution of path flow, link flow, node flow and their relevant parameters can be derived in the following *Table 1,* according to the method in the literature [13, 39].

Table 1 – Flow distribution and their parameters

Stochastic variables	Probability distribution	Mean	Variance
O-D traffic demand	$\ddot{u}^{\ddot{u}} \sim \left(\mu_q, \sigma_q\right)$	q^w	$\varepsilon^w = \rho^w q^w$
Path flow	$F_k^w \sim LN\left(\mu_{f,k}^w, \sigma_{f,k}^w\right)$	f_k^w	$\varepsilon_{f,k}^w = \rho^w f_k^w$
Link flow	$X_a \sim LN\left(\mu_{x,a}, \sigma_{x,a}\right)$	$x_a = \sum_w \sum_k f_k^w \delta_{a,k}^w$	$\varepsilon_{x,a} = \sum_w \sum_k \rho^w f_k^w \delta_{a,k}^w$
Node flow	$X_i \sim LN\left(\mu_{x,i}, \sigma_{x,i}\right)$	$x_i = \sum_w \sum_k f_k^w \delta_{i,k}^w$	$\varepsilon_{x,i} = \sum_w \sum_k \rho^w f_k^w \delta_{i,k}^w$

In *Table 1*, μ_q^w, σ_q^w, $\mu_{f,k}^w$, $\sigma_{f,k}^w$, $\mu_{x,a}$, $\sigma_{x,a}$, $\mu_{x,i}$ and $\sigma_{x,i}$ are the parameters of the lognormal distribution; $\delta_{a,k}^w$ is a binary variable, $\delta_{a,k}^w = 1$ if link a is part of path k, $\delta_{a,k}^w = 0$ otherwise; $\delta_{i,k}^w$ is a binary variable, $\delta_{i,k}^w = 1$ if the path k passes the BSS node i and battery is swapped there, $\delta_{i,k}^w = 0$ otherwise.

The travel time on the link (i.e. link travel time) is dependent on not only the links' attributes but also the traffic flow on the link, due to the traffic congestion effect. It is usually described by the link travel time function in the network equilibrium model. Here, the widely used standard BPR function is adopted [43].

$$T_a = t_a^0 \left[1 + 0.15 \cdot \left(\frac{X_a}{C_a}\right)^4\right] \tag{1}$$

where t_a^0 is the free travel time of link a, C_a is the link capacity of link a. In the travel time function, X_a is the only stochastic variables, and its n-order origin moment can be expressed as:

$$E\left[\left(X_a\right)^n\right]=exp\left[n\mu_{x,a}+\frac{n^2}{2}\left(\sigma_{x,a}\right)^2\right] \tag{2}$$

where $E[.]$ is the expectation operator. Based on *Equation 2*, the mean and variance of the link travel time can be derived as:

$$t_a=E\left(T_a\right)=t_a^0+\frac{0.15\cdot t_a^0}{\left(C_a\right)^4}E\left[\left(X_a\right)^4\right]=t_a^0\left\{1+\frac{0.15}{\left(C_a\right)^4}exp\left[4\mu_{x,a}+8\left(\sigma_{x,a}\right)^2\right]\right\} \tag{3}$$

$$\varepsilon_{t,a}=E\left[\left(T_a\right)^2\right]-\left[E\left(T_a\right)\right]^2=\left[\frac{0.15t_a^0}{\left(C_a\right)^4}\right]^2exp\left[8\mu_{x,a}+16\left(\sigma_{x,a}\right)^2\right]\left\{\exp\left[16\left(\sigma_{x,a}\right)^2\right]-1\right\} \tag{4}$$

The battery swapping service process complies with the M/M/1 queue model. The dwell time function at BSS node i adopts the following form [29, 44]:

$$T_i=t_i^0\left[1+\frac{X_i}{C_i}+\left(\frac{X_i}{C_i}\right)^2\right] \tag{5}$$

where t_i^0 is the free-flow dwell time at BSS node i, and C_i is the capacity of BSS i. In the dwell time function, X_i is the only stochastic variable, and its n-order origin moment can be expressed as:

$$E\left[\left(X_i\right)^n\right]=exp\left[n\mu_{x,i}+\frac{n^2}{2}\left(\sigma_{x,i}\right)^2\right] \tag{6}$$

Based on *Equation 6*, the mean and variance of BSS dwell time can be derived as:

$$t_i=E\left(T_i\right)=t_i^0\left[1+\frac{E\left(X_i\right)}{C_i}+\frac{E\left[\left(X_i\right)^2\right]}{\left(C_i\right)^2}\right] \tag{7}$$

$$E\left[\left(T_i\right)^2\right]=\left(t_i^0\right)^2\left\{1+\frac{2E\left(X_i\right)}{C_i}+\frac{3E\left\{\left(X_i\right)^2\right\}}{\left(C_i\right)^2}+\frac{2E\left\{\left(X_i\right)^3\right\}}{\left(C_i\right)^3}+\frac{3E\left\{\left(X_i\right)^4\right\}}{\left(C_i\right)^4}\right\} \tag{8}$$

$$\varepsilon_{t,i}=E\left[\left(T_i\right)^2\right]-\left[E\left(T_i\right)\right]^2 \tag{9}$$

Based on the assumption 4, the link travel time and dwell time at charging infrastructure are mutually independent. Then the mean travel time μ_k^w and travel time variance $\left(\sigma_k^w\right)^2$ of the path k between O-D pair w can be expressed as:

$$\mu_k^w=\sum_a\delta_{a,k}^w t_a+\sum_i\delta_{i,k}^w t_i \tag{10}$$

$$\left(\sigma_k^w\right)^2=\sum_a\delta_{a,k}^w\varepsilon_{t,a}+\sum_i\delta_{i,k}^w\varepsilon_{t,i} \tag{11}$$

According to the central limit theorem, for paths consisting of many links and nodes, the path travel time tends to follow normal distribution regardless of the link travel time distribution and BSS dwell time distribution. Travel time distribution T_k^w can be expressed as:

$$T_{\ddot{u}}^{\ddot{u}}\sim N\left(\mu\ ,\left(\sigma\ \right)^2\right) \tag{12}$$

Given confidence level α, reliable path travel time $\overline{T}_k^w$ can be decided by the following chance-constraint model [13, 39]:

$$\min\left\{\overline{T}_k^w|P\left(T_k^w\geq\overline{T}_k^w\right)\leq\alpha\right\} \tag{13}$$

By solving *Equation 13*, reliable path travel time can be expressed as expected travel time plus safety margin as follows:

$$\bar{T}_k^w = \mu_k^w + \phi^{-1}(\alpha)\sigma_k^w \tag{14}$$

where $\phi^{-1}(.)$ is the inverse of the standard normal cumulative distribution function.

2.2 Reliability-based network equilibrium model

Reviewing the literature, variational inequality (VI) is one of the main methods to build the reliability-based network equilibrium model [33, 38]. We assume that there are *m* classes of vehicles on the road network, where *m* = 0 represents GVs, and *m* = 1 represents EVs. Besides the sequence of the link, path *k* can be also written by the sequence of the sub-path denoted by *h* which connects: (1) the origin node to the destination node; (2) or the origin node to BSS node; (3) or BSS node to BSS node; (4) or BSS node to the destination node [29, 30]. The reliability-based network equilibrium model is formulated as a VI problem, which is to find a vector $f_{k,m}^{w*} \in \mathbf{\Omega}_f$, such that

$$\sum_m \sum_w \sum_k \bar{T}_{k,m}^w \left(f_{k,m}^w - f_{k,m}^{w*}\right) \geq 0 \tag{15}$$

where $\mathbf{\Omega}_f$ is the feasible path flow set defined by:

$$\sum_k f_{k,m}^w = q_m^w, \ \forall m, w \tag{16}$$

$$\left(d_k^h - D_m\right) f_{k,m}^w \leq 0, \ \forall h, k, m \tag{17}$$

$$f_{k,m}^w \geq 0, \ \forall h, k, m \tag{18}$$

$$x_{a,m} = \sum_w \sum_k f_{k,m}^w \delta_{a,k}^w \tag{19}$$

$$d_k^h = \sum_a d_a \delta_{a,k}^{w,h} \tag{20}$$

where $\bar{T}_{k,m}^w$ is the reliable travel time on path *k* of vehicles *m* between O-D pair *w*; $f_{k,m}^w$ is the flow on path *k* of vehicles *m* between O-D pair *w*; q_m^w is the traffic demand of vehicles *m* between O–D pair *w*; d_k^h is the travel distance of the sub-path *h*; D_m is the driving range of vehicles *m*; $x_{a,m}$ is the flow on link *a* of vehicles *m*; d_a is the travel distance of link *a*; $\delta_{a\,k}^h$ is a binary variable, $\delta_{a,k}^h = 1$ if link *a* is part of sub-path *h*, otherwise $\delta_{a,k}^h = 0$.

Proposition 1: the VI problem has at least one solution

Proof: According to *Equations 16–20*, the feasible path flow set $\mathbf{\Omega}_f$ is a compact convex set. Besides, according to the derivation process of reliable path travel time, $\bar{T}_{k,m}^w$ is a continuous function of the path flow $f_{k,m}^{w*}$. Based on the variational inequality theorem, the solution of the proposed VI model exists.

Proposition 1 illustrates the solution existence of the proposed model. Therefore, an efficient algorithm can be designed to solve this model, which is introduced in the next section.

Proposition 2: the VI problem is equivalent to the following network equilibrium conditions:

$$\gamma_{k,m}^w = \begin{cases} = \pi_m^w, \ if \ f_{k,m}^{w*} > 0 \\ \geq \pi_m^w, \ if \ f_{k,m}^{w*} = 0 \end{cases}, \forall w, k, m \tag{21}$$

Proof: *Equation 15* is equivalent to:

$$\sum_m \sum_w \sum_k \bar{T}_{k,m}^w f_{k,m}^w \geq \sum_m \sum_w \sum_k \bar{T}_{k,m}^w f_{k,m}^{w*}, \ \forall f_{k,m}^w \in \mathbf{\Omega}_f \tag{22}$$

Therefore, $f_{k,m}^{w*}$ is a solution to the VI model if and only if $f_{k,m}^{w*}$ is a solution of the following mathematical programming:

$$\min_{f_{k,m}^w \in \mathbf{\Omega}_f} \sum_m \sum_w \sum_k \bar{T}_{k,m}^w f_{k,m}^w \tag{23}$$

The Karush-Kuhn-Tucker (KKT) conditions for the mathematical programming could be derived as:

$$\left[\bar{T}_{k,m}^w + \sum_h \lambda_{k,m}^h \left(d_k^h - D_m\right) - \pi_m^w\right] f_{k,m}^w = 0 \tag{24}$$

$$\bar{T}_{k,m}^{w}+\sum_{h}\lambda_{k,m}^{h}\left(d_{k}^{h}-D_{m}\right)-\pi_{m}^{w}\geq 0 \tag{25}$$

where $\lambda_{k,m}^{h}$ is the Lagrange multiplier of *Equation 17*, and π_{m}^{w} is the Lagrange multiplier of *Equation 16*. Let $\gamma_{k,m}^{w}=\bar{T}_{k,m}^{w}+\sum_{h}\lambda_{k,m}^{h}\left(d_{k}^{h}-D_{m}\right)$ represent the general travel cost (GTC) on path *k* of vehicles *m* between O-D pair *w*, and π_{m}^{w} represent the minimum GTC of vehicles *m* between O-D pair *w*; then *Equations 24 and 25* can be rewritten as:

$$\left(\gamma_{k,m}^{w}-\pi_{m}^{w}\right)f_{k,m}^{w}=0 \tag{26}$$

$$\gamma_{k,m}^{w}-\pi_{m}^{w}\geq 0 \tag{27}$$

It is clear that *Equations 26 and 27* are equivalent to *Equation 21*.

Therefore, the VI problem describes such a network equilibrium condition that no traveller can improve their GTC by unilaterally changing paths. In other words, all used paths of vehicles *m* between each O-D pair have equal GTC, and unused paths have higher GTC. This is an extension of the traditional Wardrop first principle, and the solution method of the network equilibrium model can be adopted to handle this problem.

3. SOLUTION ALGORITHM

In this section, the multi-criterion labelling algorithm (MLA) is proposed to solve the reliable shortest path problem, and the column-generation-based method of the successive average algorithm (CG_MSA) is proposed to solve the reliability-based network equilibrium model.

3.1 Multi-criterion labelling algorithm

One of the essential tasks in addressing the reliability-based network equilibrium problem resolves around finding the reliable shortest path. With the consideration of travel time reliability, the reliable shortest path is the path with minimum reliable travel time among all paths between the O-D pair. Here, a multi-criterion labelling algorithm is designed to find the reliable shortest path for EVs with recharge requirements, which is an extension of the work done by Tu [35].

To describe the algorithm better, some notations and definitions should be introduced first. The link set, node set and BSS node set on the road network are respectively denoted as *A, N* and *C*. *D* is the driving range of EVs. The set of all non-dominated paths from origin node *r* to node *i* is denoted as p^{ri}, and the corresponding label set is defined as L^{ri}. For the path $p_{u}^{ri}\in P^{ri}$, its multi-criterion label is denoted as $L_{u}^{ri}\in L^{ri}$ and $L_{u}^{ri}=\left(F_{u}^{ri},t_{u}^{ri},\sigma_{u}^{ri},d_{u}^{ri}\right)$, and F_{u}^{ri}, t_{u}^{ri}, σ_{u}^{ri} and d_{u}^{ri} respectively represent reliable travel time, expected travel time, standard deviation of travel time and travel distance of the path p_{u}^{ri}. To compare the paths in the path sets, the non-dominated path is defined as follows.

Definition 1. For two paths $p_{u}^{ri},p_{v}^{ri}\in P^{ri}$, if and only if $F_{u}^{ri}\leq F_{v}^{ri}$, $t_{u}^{ri}\leq t_{v}^{ri}$ and $d_{u}^{ri}\leq d_{v}^{ri}$, and at least one of the inequalities is strict, then p_{u}^{ri} dominates p_{v}^{ri} or p_{v}^{ri} is dominated by p_{u}^{ri}, denoted as $p_{u}^{ri}\quad p_{v}^{ri}$.

Definition 2. The path $p_{u}^{ri}\in P^{ri}$ is a non-dominated path, if and only if it is not dominated by any other path $p_{v}^{ri}\in P^{ri}$.

An illustrative example is used to show how to compare the paths using Definition 1 and Definition 2. There are three paths (i.e. p_{1}^{ri}, p_{2}^{ri}, and p_{3}^{ri}) in the path set P^{ri}, and their multi-criterion labels are respectively $L_{1}^{ri}=\left(F_{1}^{ri}=12,t_{1}^{ri}=10,\sigma_{1}^{ri}=2,d_{1}^{ri}=9\right)$, $L_{2}^{ri}=\left(F_{2}^{ri}=11,t_{2}^{ri}=8,\sigma_{2}^{ri}=3,d_{2}^{ri}=8\right)$ and $L_{3}^{ri}=\left(F_{3}^{ri}=10,t_{3}^{ri}=7,\sigma_{3}^{ri}=3,d_{3}^{ri}=10\right)$. Based on Definition 1, p_{1}^{ri} is dominated by p_{2}^{ri}, because we have $F_{2}^{ri}<F_{1}^{ri}$, $t_{2}^{ri}<t_{1}^{ri}$ and $d_{2}^{ri}<d_{1}^{ri}$. Another result based on Definition 1 is that p_{2}^{ri} and p_{3}^{ri} are not dominated by any other path in p^{ri}. Therefore, p_{2}^{ri} and p_{3}^{ri} are both non-dominated paths based on Definition 2.

Two sets are introduced to store the non-dominated labels (namely the non-dominated paths) in the algorithm process. One is the set **S1** which stores the non-dominated labels that have not been extended at all nodes, and the other set **S2** stores all the non-dominated labels at all nodes. There are three main processes in the multi-criterion labelling algorithm, namely node selection, path extension and label update. The process of the multi-criterion labelling algorithm is presented as follows to find the reliable shortest path from origin node *r* to destination node *s*.

Step 1: **Initialisation.**
Let $\mathbf{S1}(r)=\mathbf{S2}(r)=L^{rr}=\{(0,0,0,0)\}$, and $\mathbf{S1}(i)=\mathbf{S2}(i)=L^{ri}=\emptyset,\forall i\in N\setminus\{r\}$.

Step 2: **Node selection.**
If $\mathbf{S1}(i)=\emptyset,\forall i\in N,$ then stop; otherwise, continue.
From all nodes in N, select the node i with the minimum $F_{min}^{ri}=min\left(F_1^{ri}\ldots F_u^{ri}\ldots\right)$.
If $i=s$ then stop; otherwise, continue.

Step 3: **Path extension.**
For all links $a_{ij}\in A$,
If $j\notin C$, then let $\hat{L}^{rj}=\mathbf{S1}(i)\oplus a_{ij}$, and if $d_u^{rj}>D$, delete label $\hat{L}_u^{rj}$ in $\hat{L}^{rj}$.
If $j\in C$, then let $\hat{L}^{rj}=\mathbf{S1}(i)\boxplus a_{ij}$, and if $d_u^{rj,1}>D$, delete labels $\hat{L}_u^{rj,1}$ and $\hat{L}_u^{rj,2}$ in $\hat{L}^{rj}$.
Then let **S1**(i)=∅.

Step 4: **Label update.**
Merge the label set $\overline{L}^{rj}$ and $\hat{L}^{rj}$, and obtain the new non-dominated label set $\overline{L}^{rj}$.
Let $L^{rj}=\overline{L}^{rj}$, $\mathbf{S2}(j)=L^{rj}$, and $\mathbf{S1}(j)=L^{rj}\cap\left(\mathbf{S1}(j)\cup\hat{L}^{rj}\right)$, turn to step 2.

In step 2, there are two termination criteria. One is $\mathbf{S1}(i)=\emptyset$, which means no non-dominated paths can be extended. The other is that the node with the minimum F_{min}^{ri} among all nodes in N is node s, which means the reliable shortest path from node r to node s is found. If any termination criterion is satisfied, the algorithm ends; otherwise, the node with the minimum F_{min}^{ri} is selected for path extension.

In step 3, non-dominated paths are extended to the adjacent nodes of the selected node in step 2. There are two operators in the process of path extension. $\mathbf{S1}(i)\oplus a_{ij}$ means that every path p_u^{ri} stored in **S1**(i) is extended to node j passing link $a_{ij}\in\mathrm{A}$ with attributes $\left(t_{ij},\sigma_{ij},d_{ij}\right)$, and the new path p_u^{rj} is generated with the label $\hat{L}_u^{rj}=\left(\hat{F}_u^{rj},\hat{t}_u^{rj},\hat{\sigma}_u^{rj},d_u^{rj}\right)$, in which $\hat{F}_u^{rj}=\hat{t}_u^{rj}+\phi^{-1}(\alpha)\hat{\sigma}_u^{rj}$, $\hat{t}_u^{rj}=t_u^{ri}+t_{ij}$, $\hat{\sigma}_u^{rj}=\sqrt{\left(\sigma_u^{ri}\right)^2+\left(\sigma_{ij}\right)^2}$ $\hat{d}_u^{rj}=d_u^{ri}+d_{ij}$. $\mathbf{S1}(i)\boxplus a_{ij}$ means that every path p_u^{ri} stored in **S1**(i) is extended to node j passing link $a_{ij}\in\mathrm{A}$ with attributes $\left(t_{ij},\sigma_{ij},d_{ij}\right)$ and BSS node $j\in C$ with attributes $\left(t_j,\sigma_j\right)$, and two new paths $p_u^{rj,1}$ and $p_u^{rj,2}$ are generated. The path $p_u^{rj,1}$ has no battery swapping action at BSS node j, and its corresponding label is $\hat{L}_u^{rj,1}=\left(\hat{F}_u^{rj,1},\hat{t}_u^{rj,1},\hat{\sigma}_u^{rj,1},d_u^{rj,1}\right)$, in which $\hat{F}_u^{rj,1}=\hat{t}_u^{rj,1}+\phi^{-1}(\alpha)\hat{\sigma}_u^{rj,1}$, $\hat{t}_u^{rj,1}=t_u^{ri}+t_{ij}$, $\hat{\sigma}_u^{rj}=\sqrt{\left(\sigma_u^{ri}\right)^2+\left(\sigma_{ij}\right)^2}$, $\hat{d}_u^{rj,1}=d_u^{ri}+d_{ij}$; the path $p_u^{rj,2}$ has battery swapping action at BSS node j, and its corresponding label is $\hat{L}_u^{rj,2}=\left(\hat{F}_u^{rj,2},\hat{t}_u^{rj,2},\hat{\sigma}_u^{rj,2},d_u^{rj,2}\right)$, in which $\hat{F}_u^{rj,2}=\hat{t}_u^{rj,2}+\phi^{-1}(\alpha)\hat{\sigma}_u^{rj,2}$, $\hat{t}_u^{rj,2}=t_u^{ri}+t_{ij}+t_j$, $\hat{\sigma}_u^{rj,2}=\sqrt{\left(\sigma_u^{ri}\right)^2+\left(\sigma_{ij}\right)^2+\left(\sigma_j\right)^2}$, $\hat{d}_u^{rj,2}=0$. However, if $\hat{d}_u^{rj}>D$ or $\hat{d}_u^{rj,1}>D$, the corresponding paths are not feasible, and their labels should be deleted. Because **S1** only stores the unextended non-dominated labels, **S1**(i) should be set as ∅ after the path extension.

In step 4, the new label set $\hat{L}^{rj}$ generated by the path extension and the current label set L^{rj} at node j are merged as the label set $\overline{L}^{rj}$ with the path-by-path comparison based on Definition 1 and Definition 2. Then the set of all non-dominated labels L^{rj} is updated by $\overline{L}^{rj}$ and stored in **S2**(j). The set of unextended non-dominated labels is updated and stored in **S1**(j) by set operation. In detail, $\mathbf{S1}(j)\cup\hat{L}^{rj}$ represents the set of all unextended labels in which there may be some dominated labels, and L^{rj} includes all non-dominated labels, then $L^{rj}\cap\left(\mathbf{S1}(j)\cup\hat{L}^{rj}\right)$ presents the set of unextended non-dominated labels.

3.2 Column-generation-based method of successive average algorithm

The MSA algorithm has been widely used to solve the network equilibrium model, due to its simplicity and the forced convergence property [45]. Based on the proposed MLA algorithm, the MSA algorithm is considered to be incorporated into the column generation framework. The main idea is to generate an updatable working path set, which is used to store the paths that travellers may choose. In each iteration, the working path set is updated by the reliable shortest path for each O-D pair solved by the MLA algorithm, and the network equilibrium is solved in the updated working path set by the MSA algorithm. When updated working paths have little or no impact on the link flow pattern, the convergence condition is met, and the algorithm ends. It ensures that all used paths are included in the working path set, and an effective working path set can be generated after the algorithm is finished. The process of the CG_MSA algorithm is presented as follows:

Step 1: Initialisation. Based on the free-flow travel time, find the shortest path for each class of vehicles between all O-D pairs, generate the working path set $\mathbf{RS}_{\mathbf{m}}^{0}$, perform all-or-nothing assignment to obtain the initial flow vector $\mathbf{x}^{0}$ (including link and node flow), set the outer iteration counter $nn = 0$ and the outer tolerance error e_{out}.

Step 2: **Update link and node travel time**. Based on the flow vector $\mathbf{x}^{(nn)}$, update the mean and variance of link and node travel time.

Step 3: **Update working path set**. Based on the current link and node travel time, find the reliable shortest path for each class of vehicles between all O-D pairs using MLA, and update the working path set $\mathbf{RS}_{\mathbf{m}}^{\mathbf{nn}+1}$.

Step 4: **Perform network equilibrium in the working path set.**
Step 4.1: **Initial network loading**. Based on the free-flow travel time, perform all-or-nothing assignment and obtain the initial path flow vector $\mathbf{f}^{0}$, set the inner iteration counter $n = 0$ and the inner tolerance error e_{in}.
Step 4.2: **Update reliable path travel time.** Based on the path flow, obtain the link and node flow, according to *Equation 14*, update the reliable path travel time.
Step 4.3: **Find the search direction**. Compare the reliable travel time of all paths and find the minimum one for each O-D pair, perform all-or-nothing assignment and obtain the auxiliary path flow $\mathbf{f}^{(n)'}$.
Step 4.4: **Update the path flow**. Update the path flow $\mathbf{f}^{(n+1)} = \mathbf{f}^{(n)} + 1/n\left(\mathbf{f}^{(n)'} - \mathbf{f}^{(n)}\right)$.
Step 4.5: **Convergence test.** If $\left\|\mathbf{f}^{(n+1)} - \mathbf{f}^{(n)}\right\| / \left\|\mathbf{f}^{(n)}\right\| \le e_{in}$, then stop and output $\mathbf{f}^{(n+1)}$ and the corresponding $\mathbf{x}^{(nn+1)}$; otherwise, set $n = n+1$ and go to step 4.2.

Step 5: **Convergence test.** If $\left\|\mathbf{x}^{(nn+1)} - \mathbf{x}^{(nn)}\right\| / \left\|\mathbf{x}^{(nn)}\right\| \le e_{out}$, then stop; otherwise, set $nn = nn+1$ and go to step 2.

To better illustrate the process of the CG_MSA algorithm, a flowchart is also presented as the following *Figure 2*.

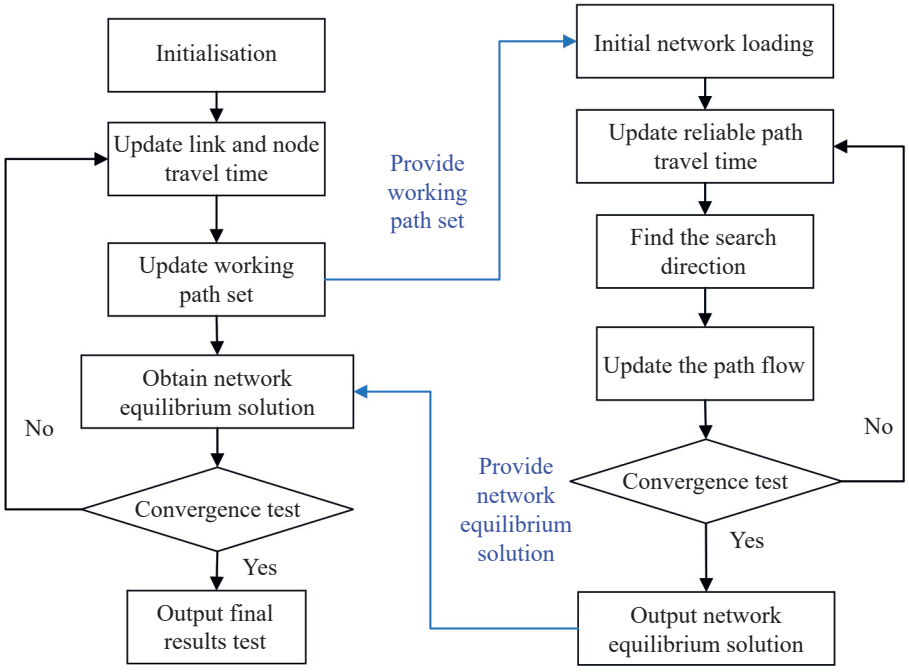

Figure 2 – The flowchart of the CG_MSA algorithm

4. NUMERICAL EXAMPLES

4.1 Nguyen-Dupuis network

The Nguyen-Dupuis network [46] is adopted to illustrate the essential idea of the proposed model, which is a widely used benchmark network for conducting numerical experiments related to network equilibrium models. As shown in *Figure 3*, this network consists of 4 O-D pairs, 13 nodes and 19 links. Due to its small scale, it is suitable to solve the proposed model and display the path-related results. For instance, all the paths in the network can be enumerated, and the working path set can be easily generated. Therefore, the steps regarding

the working path set in the algorithm can be simplified, and the details of the path-related results can be well presented.

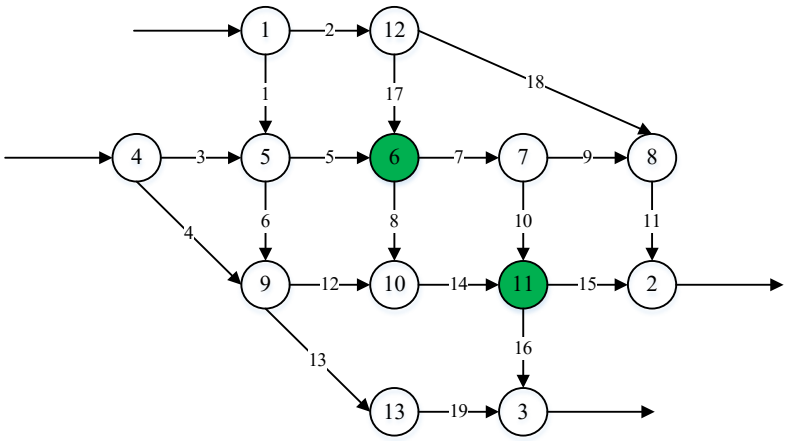

Figure 3 – The Nguyen-Dupuis network

The traffic demand for each O-D pair (1-2, 1-3, 4-2 and 4-3) is, respectively, 400 pcu/h, 800 pcu/h, 600 pcu/h and 200 pcu/h. Nodes 6 and 11 are the BSSs, their free-flow dwell time is set as 30 min, and their capacity is set as 300 pcu/h and 500 pcu/h. The link characteristics of the Nguyen-Dupuis network are shown in *Table 2.* There are 25 physical paths in the network, and if the recharge requirement is considered, there are 70 active paths in total. However, not all the paths are feasible for EVs, and the number of feasible paths will change with the driving range of EVs as shown in *Figures 4a and 4b*.

Table 2 – Link characteristics of the Nguyen-Dupuis network

Link no.	Free-flow travel time [min]	Capacity [pcu/h]	Distance [km]	Link No.	Free-flow travel time [min]	Capacity [pcu/h]	Distance [km]
1	70	900	70	11	100	700	100
2	80	700	80	12	100	700	100
3	90	700	90	13	90	600	90
4	140	900	140	14	80	700	80
5	50	800	50	15	90	700	90
6	90	600	90	16	80	700	80
7	50	900	50	17	70	300	70
8	130	500	130	18	150	700	150
9	50	300	50	19	110	700	110
10	90	400	90				

Firstly, we compare the traffic flow pattern on the road network predicted by different models. For simplicity, our proposed model is called RNE, and the network equilibrium model without considering travel time reliability (namely $\alpha = 0.5$ and $\phi^{-1}(\alpha) = 0$) is called NE. For the RNE model, the confidence level is set as $\alpha = 0.9$. There are two classes of vehicles in the network, namely EVs and GVs (the driving range is set large enough). The proportion of EVs is set as 20%, and their driving range is set as D= 300 km. The link flows and their relative difference predicted by RNE and NE are presented as *Figures 5a and 5b*. As seen in *Figure 5b*, the relative increase on link 3 is up to 14.6%, and the relative decrease on link 14 is up to -26.4%. As seen in *Figure 6*, the node flow at BSS node 6 increases from 163 pcu/h to 182 pcu/h, and the node flow at BSS node 11 decreases from 237 pcu/h to 218 pcu/h.

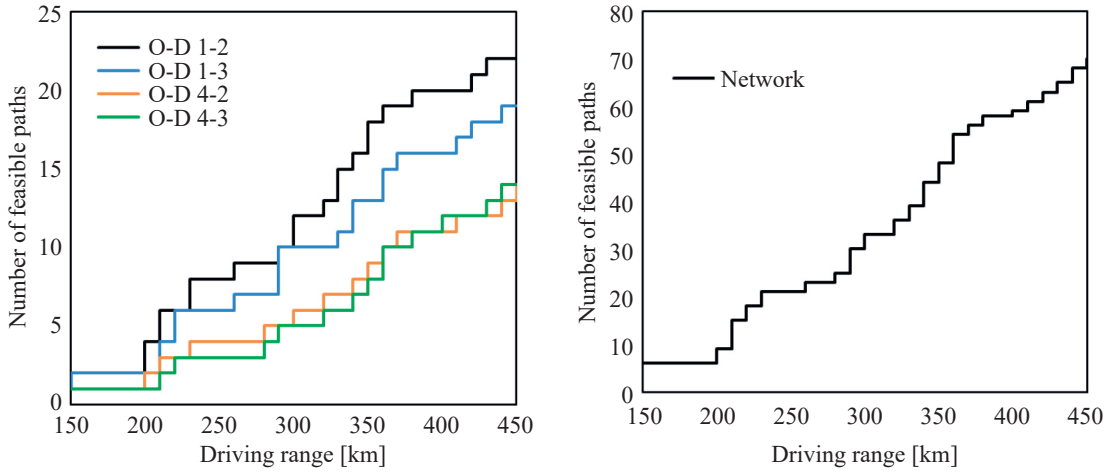

a) Number of feasible paths for O-D pairs *b) Number of feasible paths for the network*

Figure 4 – Number of feasible paths for EVs

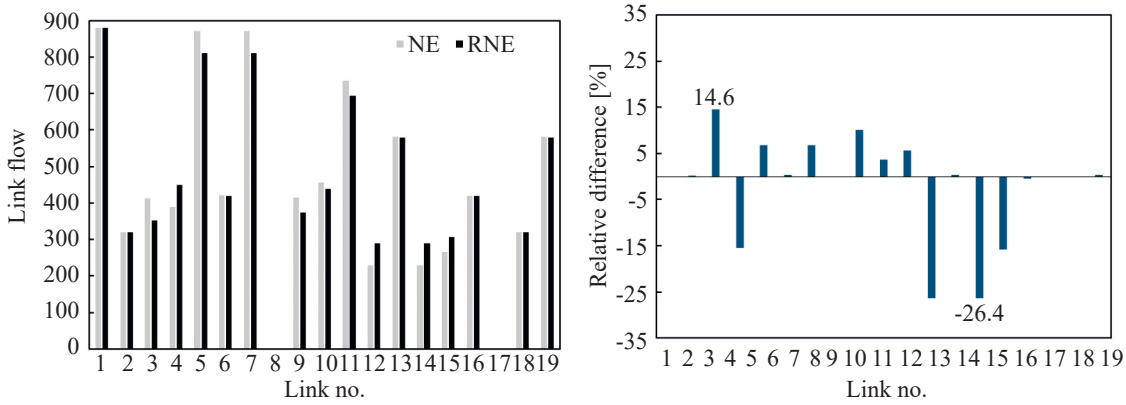

a) Link flow predicted by RNE and NE *b) Relative difference of link flow predicted by RNE and NE*

Figure 5 – Comparison of link flow predicted by RNE and NE

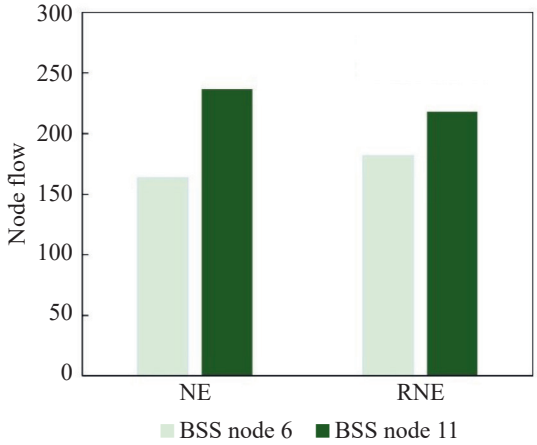

Figure 6 – Comparison of node flow predicted by RNE and NE

Following that, the path-related results of O-D pair 3 (4-2) are selected for illustration. The path flow, expected travel time, safety margin and reliable travel time of these paths for EVs and GVs in the RNE model are listed in the following *Table 3*. In the node sequence, $\overline{n}$ means EVs have battery swapping action at BSS node $\overline{n}$. In this O-D pair, there are 6 and 5 feasible paths for EVs and GVs. However, at the equilibrium state, there are only 4 used paths for them (2 paths for EVs and 2 paths for GVs). The cumulative probability distribution of paths' travel time can be seen in *Figure 7*. According to the results, it is clear that travellers care

about both expected travel time and travel time reliability when making path choices. Because the results of EVs and GVs are similar, we take the results of GVs as an example. Though GV Path 4 has a higher expected travel time than GV Path 1 and GV Path 2, its travel time variance and safety margin are very low, so there are still many travellers choosing GV Path 4 with the consideration of travel time reliability. For GV Path 2, though it has a lower expected travel time than GV Path 4, its travel time variance and safety margin are much higher, and there are no travellers choosing it. Besides, we can also find that the reliable travel time of GV Path 1 and GV Path 4 is shorter than that of other paths at the equilibrium state.

Table 3 – Path-related results of O-D par 3 in RNE model

Vehicle type	Path no.	Node sequence	Path flow	Expected travel time	Safety margin	Reliable travel time
EVs	1	4-5-$\overline{6}$-7-8-2	102.71	451.51	26.21	477.72
	2	4-5-$\overline{6}$-7-11-2	0.00	467.55	23.50	491.05
	3	4-5-6-7-$\overline{11}$-2	17.26	456.79	20.96	477.75
	4	4-5-$\overline{6}$-7-$\overline{11}$--2	0.00	516.61	24.51	541.12
	5	4-5-$\overline{6}$-10-11-2	0.03	510.41	13.75	524.16
	6	4-5-$\overline{6}$-10-$\overline{11}$-2	0.00	559.47	15.41	574.88
GVs	1	4-5-6-7-8-2	191.49	391.69	22.92	414.61
	2	4-5-6-7-11-2	0.00	407.73	19.77	427.50
	3	4-5-6-10-11-2	0.00	450.59	5.25	455.84
	4	4-9-10-11-2	288.51	413.04	1.57	414.61
	5	4-5-9-10-11-2	0.00	456.31	3.52	459.83

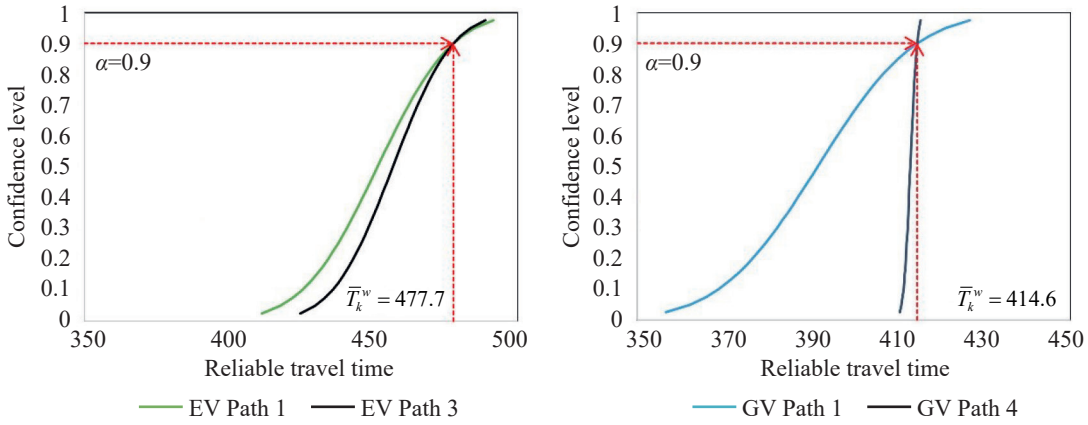

Figure 7 – Cumulative probability distribution of paths' travel time

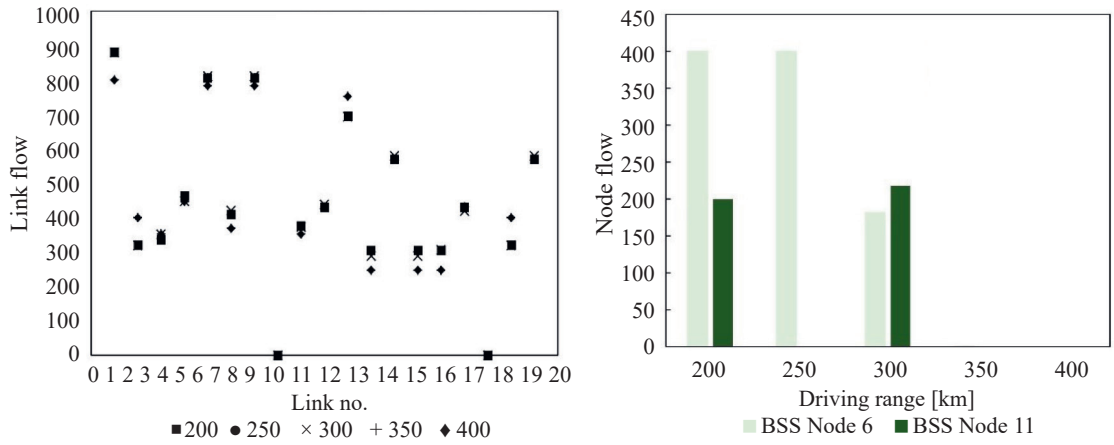

a) The influence of driving range on link flow *b) The influence of driving range on node flow*

Figure 8 – The influence of driving range on traffic flow pattern

The driving range is one of the key factors affecting the path choice of EVs. The driving range is respectively set as 200 km, 250 km, 300 km, 350 km and 400 km to analyse its influence on traffic flow pattern. As *Figure 8a* shows, the link flow on the road network changes with the variation of driving range. As *Figure 8b* shows, when the driving range is 200 km EVs between O-D pairs 1-3 and 4-3 need to swap battery twice to reach destinations, so the total node flow exceeds the number of EV traffic demand and reaches 600 pcu/h; when the driving range is 250 km, all EVs only need to swap battery once to reach destinations, but the BSS node 11 is too far from the origin node, so all EVs swap battery at BSS node 6; when the driving range reaches 300 km, which covers the distance from all origin nodes to BSS node 11, both of BSS nodes attract some EVs to swap battery; when the driving range is not lower than 350 km, EVs can reach the destination without en-route battery swapping, so the node flow on both BSS nodes is 0.

4.2 Sioux Falls network

The Sioux Falls network, which consists of 552 O-D pairs, 24 nodes and 76 links, is adopted to test the applicability of the proposed model and algorithm, as shown in *Figure 9*. The parameters of the network such as the O-D traffic demand and link capacity are the same as those in the reference [47]. To simulate the medium-distance or long-distance travel scene, the free-flow travel time of the link is expanded to 10 times as that in the reference [47], and the distance of the link is set to twice its free-flow travel time. In this context, the free-flow travel speed is 120 km/h, and the shortest travel distances of O-D pairs are distributed within the range of [24km, 276km]. There are 4 BSS nodes in this network, whose characteristics are shown in *Table 4*. There are two classes of vehicles in the network, namely EVs and GVs. The proportion of EVs is set as 20%, and their driving range is set as D=200 km. The variance-to-mean ratio is set as $\rho^w = 10$, and the confidence level is set as $\alpha = 0.9$. The values of these parameters are set for case illustration, and they can be further calibrated by survey data in practical applications.

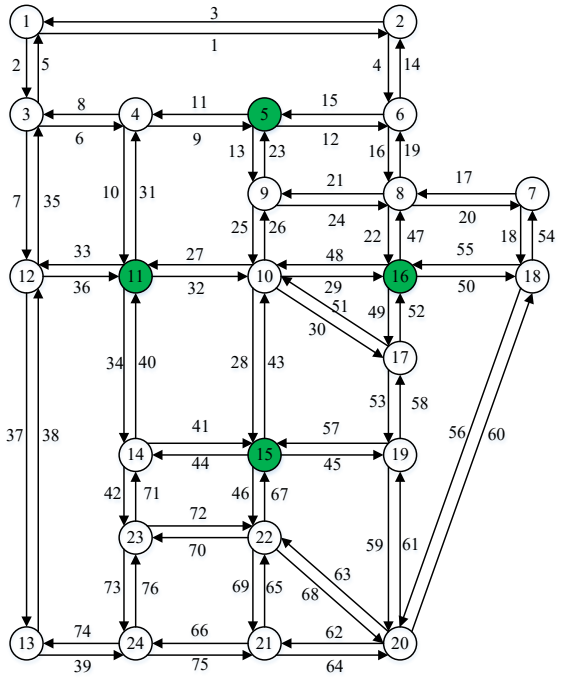

Figure 9 – The Sioux Falls network

Table 4 – Characteristics of BSS nodes

BSS nodes	Free-flow dwell time [min]	Capacity [pcu/h]
5	20	8000
11	30	6000
15	30	6000
16	20	8000

Firstly, the convergence process of the CG_MSA algorithm is illustrated. As *Figure 10* shows, the proposed algorithm can converge to an ideal error with only 5 outer iterations. For the inner iteration with the given working path set at the last outer iteration, the algorithm approaches the convergence error 10^{-3} at 235 iterations and 10^{-4} at 1771 iterations.

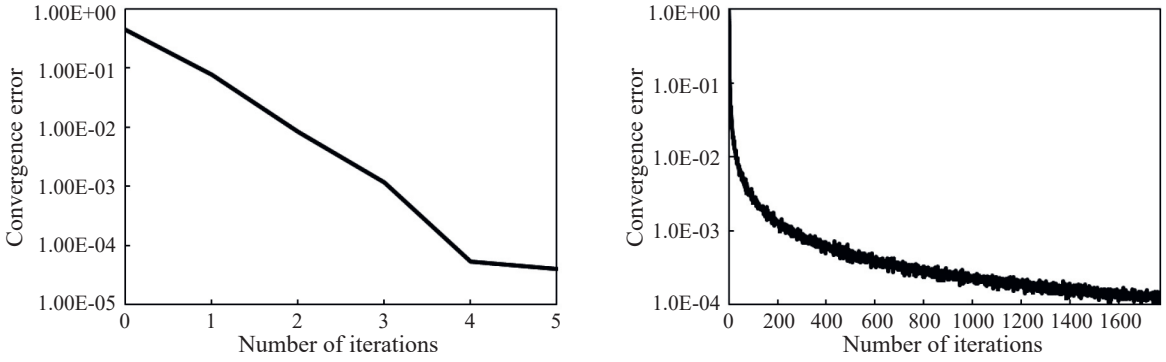

a) Convergence process of outer iteration *b) Convergence process of inner iteration*

Figure 10 – Convergence process of CG_MSA algorithm

Following that, the convergence process of working paths' reliable travel time is illustrated. The working paths of O-D pair 10-24 is selected as the example. There are 4 working paths for GVs, which are Path 1: 10-15-22-21-24, Path 2: 10-15-14-23-24, Path 3: 10-11-14-23-24, Path 4: 10-15-22-23-4. There are 2 working paths for EVs, which are Path 1: 10-$\overline{15}$-22-21-24, Path 2: 10-$\overline{15}$-22-23-24. As *Figure 11* shows, the reliable travel time of all GVs' working paths converges to 427 minutes, and the reliable travel time of all EVs' working paths converges to 549 minutes. It illustrates that the results satisfy the network equilibrium conditions, and the CG_MSA algorithm is practical and effective.

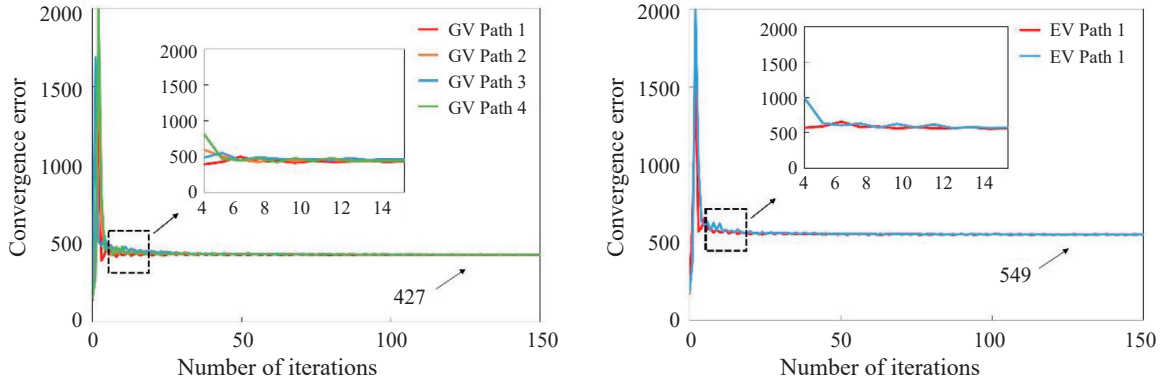

a) Convergence process of working paths' reliable travel time for GVs *b) Convergence process of working paths' reliable travel time for EVs*

Figure 11 – Convergence process of working paths' reliable travel time

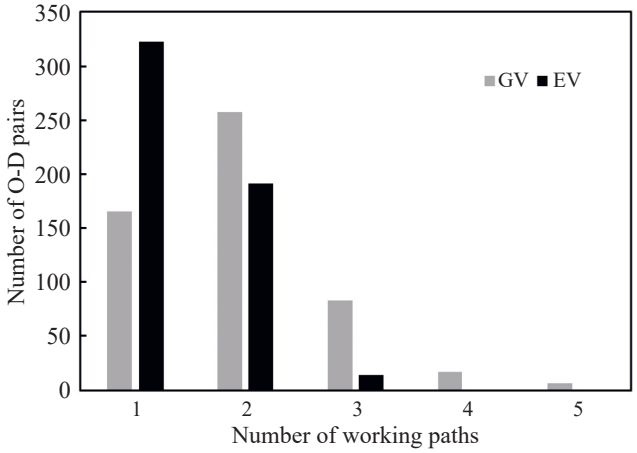

Figure 12 – The number distribution of working paths for O-D pairs

Finally, the working path set generated by the CG_MSA algorithm is analysed. The working path set totally consists of 1773 working paths, in which there are 747 working paths for EVs and 1026 working paths for GVs. The number distribution of working paths for O-D pairs is shown in *Figure 12*. It can be seen that the number of EVs' working paths for each O-D pair is no more than 3, and that of GVs' is no more than 5.

5. CONCLUSIONS

This paper presents a reliability-based network equilibrium model to predict the traffic flow pattern on the road network with EVs and GVs, in which travel time reliability, EVs' driving range and recharge requirements are all considered. The derivation of reliable path travel time is presented, and the reliability-based network equilibrium model is formulated as a VI problem. The existence of solutions and equivalent equilibrium conditions are analysed for the proposed model. Then the MLA algorithm is proposed to solve the reliable shortest path problem, and the CG_MSA algorithm is proposed to solve the reliability-based network equilibrium model.

The effectiveness and applicability of the proposed model and algorithm are verified on the Nguyen-Dupuis network and Sioux Falls network. The analysis results indicated that: (1) travel time reliability has a great influence on the traffic flow pattern on the road network, the relative difference of link flow on the Nguyen-Dupuis network predicted by different models is up to -26.4%; (2) travellers' path choice is affected by travel time reliability, travellers will choose the path with high expectation time but low travel time variance to ensure their reliable travel time is optimal; (3) the driving range of EVs affects the en-route recharge requirement of travellers, and the link flow and node flow will both change greatly with the variance of EVs' driving range; (4) the proposed algorithm can quickly converge to the equilibrium conditions and it is applicable to the real city network. As these results conclude, our proposed model and algorithm can capture the travel time reliability and EVs' travel behaviour, which present a more accurate traffic flow pattern. Benefiting from the flexibility of the proposed model, the method can be easily extended to other regions and cities by using corresponding traffic demand and road network data.

However, there are some limitations in our study that need to be further studied in the future. First, the values of some parameters are assumed for illustration, for example the parameters of traffic demand and travel time distribution, which should be calibrated by actual survey data. Second, this problem is studied in the UE framework, which assumes travellers are rational and have perfect information regarding travel time over the entire network. However, we can extend it to the bounded rational user equilibrium and stochastic user equilibrium with the consideration of travellers' bounded rationality and perceived error. Third, the uncertainty of the transportation system is assumed to mainly come from the stochastic traffic demand in this study, and other uncertainty sources can be further studied, for example road capacity and EVs' driving range. Lastly, considering travellers' feedback on the charging infrastructure location, our proposed model can be used to optimise the charging infrastructure location in a bi-level programming framework.

ACKNOWLEDGMENT

This study is supported by the Project of Chongqing Social Science Planning (2022BS082), the Science and Technology Research Program of Chongqing Municipal Education Commission (KJQN202100715), the Science and Technology Research Program of Chongqing Jiaotong University (21JDKJC-A016), the Project of Chongqing Construction Technology Plan (the management service platform of urban dynamic and static traffic integration), the Open Fund Project of Chongqing Key Laboratory of Traffic & Transportation (2018TE01).

REFERENCES

[1] Kumar RR, Alok K. Adoption of electric vehicle: A literature review and prospects for sustainability. *Journal of Cleaner Production*. 2020;253:119911. DOI: 10.1016/j.jclepro.2019.119911.

[2] IEA. *Global EV Outlook 2022*. https://www.iea.org/reports/global-ev-outlook-2022. html.

[3] CleanTechnica. *31 Countries, States, And Cities Have Gas/Diesel Car Bans In Place*. https://cleantechnica.com/2021/01/02/31-countries-states-and-cities-have-ice-bans-in-place/.

[4] Hu Y, et al. The Chinese plug-in electric vehicles industry in post-COVID-19 era towards 2035: Where is the path to revival? *Journal of Cleaner Production*. 2022;361:132291. DOI: 10.1016/j.jclepro.2022.132291.

[5] Li M, et al. Network traffic flow evolution with battery electric vehicles and conventional gasoline vehicles. *Journal of Southeast University (English Edition)*. 2019;35(2):213-219. DOI: 10.3969/j.issn.1003-7985.2019.02.011.

[6] Tu Q, et al. Stochastic transportation network considering ATIS with the information of environmental cost. *Sustainability*. 2018;10(11):3861. DOI: 10.3390/su10113861.

[7] Tu Q, et al. Traffic paradox under different equilibrium conditions considering elastic demand. *Promet – Traffic&Transportation*. 2019;31(1):1-9. DOI: 10.7307/PTT.V31I1.2795.

[8] Sheffi Y. Urban transportation networks.Englewood Cliffs, NJ: Prentice-Hall. 1985.

[9] Zhu S, Levinson D. Do people use the shortest path? An empirical test of Wardrop's first principle. *PloS one.* 2015;10(8):e0134322. DOI: 10.1371/journal.pone.0134322.

[10] Maher M. Algorithms for logit-based stochastic user equilibrium assignment. *Transportation Research Part B: Methodological*. 1998;32(8):539-549. DOI: 10.1016/S0191-2615(98)00015-0.

[11] Prashker JN, Bekhor S. Route choice models used in the stochastic user equilibrium problem: A review. *Transport reviews*. 2004;24(4):437-463. DOI: 10.1080/0144164042000181707.

[12] Huang HJ, Lam WHK. Modeling and solving the dynamic user equilibrium route and departure time choice problem in network with queues. *Transportation Research Part B: Methodological*. 2002;36(3):253-273. DOI: 10.1016/S0191-2615(00)00049-7.

[13] Shao H, et al. A reliability-based stochastic traffic assignment model for network with multiple user classes under uncertainty in demand. *Networks and Spatial Economics*. 2006;6:173-204. DOI: 10.1007/s11067-006-9279-6.

[14] Wang L, et al. A reliability-based traffic equilibrium model with boundedly rational travelers considering acceptable arrival thresholds. *Sustainability*. 2023;15(8):6988. DOI: 10.3390/su15086988.

[15] Yan D, Guo J. A Multiclass cumulative prospect theory-based stochastic user equilibrium model with path constraints in degradable transport networks. *Promet – Traffic&Transportation*. 2021;33(5):775-787. DOI: 10.7307/PTT.V33I5.3586.

[16] Dafermos S. The general multimodal network equilibrium problem with elastic demand. *Networks*. 1982;12(1):57-72. DOI: 10.1002/net.3230120105.

[17] Ge Y, MacKenzie D. Charging behavior modeling of battery electric vehicle drivers on long-distance trips. *Transportation Research Part D: Transport and Environment*. 2022;113:103490. DOI: 10.1016/j.trd.2022.103490.

[18] Mansfield C, et al. An efficient detour computation scheme for electric vehicles to support smart cities' electrification. *Electronics*. 2022;11(5):803. DOI: 10.3390/electronics11050803.

[19] Ma J, et al. Stochastic electric vehicle network considering environmental costs. *Sustainability*. 2018;10(8):2888. DOI: 10.3390/su10082888.

[20] Ma J, Wang H, Tang T. Stochastic electric vehicle network with elastic demand and environmental costs. *Journal of Advanced Transportation*. 2020;2020:1-11. DOI: 10.1155/2020/4169826.

[21] Ahn K, et al. Multi-objective eco-routing model development and evaluation for battery electric vehicles. *Transportation Research Record*. 2021;2675(12):867-879. DOI: 10.1177/03611981211031529.

[22] Ma J, et al. Analysis of urban electric vehicle adoption based on operating costs in urban transportation network. *Systems*. 2023;11(3):149. DOI: 10.3390/systems11030149.

[23] Jiang N, Xie C, Waller ST. Path-constrained traffic assignment: model and algorithm. *Transportation Research Record*. 2012;2283(1):25-33. DOI: 10.3141/2283-03.

[24] Jiang N, Xie C. Computing and analyzing mixed equilibrium network flows with gasoline and electric vehicles. *Computer-Aided Civil and Infrastructure Engineering*. 2014;29(8):626-641. DOI: 10.1111/mice.12082.

[25] Jing W, et al. Stochastic traffic assignment of mixed electric vehicle and gasoline vehicle flow with path distance constraints. *Transportation Research Procedia*. 2017;21:65-78. DOI: 10.1016/j.trpro.2017.03.078.

[26] Jing W, et al. Location design of electric vehicle charging facilities: A path-distance constrained stochastic user equilibrium approach. *Journal of Advanced Transportation*. 2017. DOI: 10.1155/2017/4252946.

[27] Xie C, Jiang N. Relay requirement and traffic assignment of electric vehicles. *Computer-Aided Civil and Infrastructure Engineering*. 2016;31(8):580-598. DOI: 10.1111/mice.12193.

[28] He F, Yin Y, Lawphongpanich S. Network equilibrium models with battery electric vehicles. *Transportation Research Part B: Methodological*. 2014;67:306-319. DOI: 10.1016/j.trb.2014.05.010.

[29] Xu M, Meng Q, Liu K. Network user equilibrium problems for the mixed battery electric vehicles and gasoline vehicles subject to battery swapping stations and road grade constraints. *Transportation Research Part B: Methodological*. 2017;99:138-166. DOI: 10.1016/j.trb.2017.01.009.

[30] Zhang X, et al. Range-constrained traffic assignment with multi-modal recharge for electric vehicles. *Networks and Spatial Economics*. 2019;19(2):633-668. DOI: 10.1007/s11067-019-09454-9.

[31] Asakura Y, Kashiwadani M. Road network reliability caused by daily fluctuation of traffic flow. *19th PTRC Summer Annual Meeting, 1991, University of Sussex, United Kingdom*. 1991.

[32] Gu Y, et al. Performance of transportation network under perturbations: Reliability, vulnerability, and resilience. *Transportation Research Part E: Logistics and Transportation Review*. 2020;133:101809. DOI: 10.1016/j.tre.2019.11.003.

[33] Sun C, Cheng L, Ma J. Travel time reliability with boundedly rational travelers. *Transportmetrica A: Transport Science*. 2017;14(3):210-229. DOI: 10.1080/23249935.2017.1368733.

[34] Senna LADS. The influence of travel time variability on the value of time. *Transportation*. 1994;21:203-228. DOI: 10.1007/bf01098793.

[35] Tu Q, et al. The constrained reliable shortest path problem for electric vehicles in the urban transportation network. *Journal of Cleaner Production*. 2020;261:121130. DOI: 10.1016/j.jclepro.2020.121130.

[36] Ruß M, Gust G, Neumann D. The constrained reliable shortest path problem in stochastic time-dependent networks. *Operations Research*. 2021;69(3):709-726. DOI: 10.1287/opre.2020.2089.

[37] Shen L, et al. An energy-efficient reliable path finding algorithm for stochastic road networks with electric vehicles. *Transportation Research Part C: Emerging Technologies*. 2019;102:450-473. DOI: 10.1016/j.trc.2019.03.020.

[38] Shen L, et al. A reliability-based stochastic traffic assignment model for signalized traffic network with consideration of link travel time correlations. *Sustainability*. 2022;14(21):14520. DOI: 10.3390/su142114520.

[39] Chen A, Zhou Z. The α-reliable mean-excess traffic equilibrium model with stochastic travel times. *Transportation Research Part B: Methodological*. 2010;44(4):493-513. DOI: 10.1016/j.trb.2009.11.003.

[40] Sun C, et al. Day-to-day traffic user equilibrium model considering influence of intelligent highways and advanced traveler information systems. *Journal of Central South University*. 2022;29(4):1376-1388. DOI: 10.1007/s11771-022-4974-0.

[41] Tao Y, et al. Review of optimized layout of electric vehicle charging infrastructures. *Journal of Central South University*. 2021;28(10):3268-3278. DOI: 10.1007/s11771-021-4842-3.

[42] Zhan W, et al. A review of siting, sizing, optimal scheduling, and cost-benefit analysis for battery swapping stations. *Energy*. 2022;124723. DOI: 10.1016/j.energy.2022.124723.

[43] Ma J, et al. Link restriction: Methods of testing and avoiding braess paradox in networks considering traffic demands. *Journal of Transportation Engineering, Part A: Systems*. 2018;144(2):04017076. DOI: 10.1061/jtepbs.0000111.

[44] Zhang TY, et al. Deploying public charging stations for battery electric vehicles on the expressway network based on dynamic charging demand. *IEEE Transactions on Transportation Electrification*. 2022;8(2):2531-2548. DOI: 10.1109/tte.2022.3141208.

[45] Wang D, et al. A generalized mean-variance metric of route choice model under travel time uncertainty. *Transportmetrica A: Transport Science*. 2022;18(2):299-323. DOI: 10.1080/23249935.2020.1773573.

[46] Nguyen S, Dupuis C. An efficient method for computing traffic equilibria in networks with asymmetric transportation costs. *Transportation Science*. 1984;18(2):185-202. DOI: 10.1287/trsc.18.2.185.

[47] Stabler B. Transportation networks for research. 2020. https://github.com/bstabler/TransportationNetworks.

涂强，李嫚嫚，吴永军

混入电动汽车和燃油汽车的可靠网络均衡模型

摘要：随着电动汽车的普及，它们已经成为道路网络交通流中不可缺少的一部分。为实现电动汽车和燃油汽车混合道路网络的交通流分布预测，提出了一种基于可靠性的网络均衡模型，该模型考虑了出行时间可靠性、电动汽车续航里程和充电需求。推导了可靠路径出行时间的数学表达式，并将基于可靠性的网络均衡模型表述为一个变分不等式问题。然后，提出一种多准则标号算法来求解可靠最短路径问题，并提出一种基于列生成的相继平均算法来求解基于可靠性的网络均衡模型。在Nguyen-Dupuis路网和Sioux Falls城市路网中验证了模型和算法的适用性和有效性。本文的模型和算法可以推广到其他路网，帮助交通管理者分析交通状况，制定可持续的交通政策。

关键词：交通运输工程，可靠网络均衡，电动汽车，续航里程，充电需求